Edward M. Suzuki,[1] *Ph.D. and Mike Carrabba,*[2] *Ph.D.*

In Situ Identification and Analysis of Automotive Paint Pigments Using Line Segment Excitation Raman Spectroscopy: I. Inorganic Topcoat Pigments[3]

REFERENCE: Suzuki EM, Carrabba M. In situ identification and analysis of automotive paint pigments using line segment excitation Raman spectroscopy: I. Inorganic topcoat pigments. J Forensic Sci 2001;46(5):1053–1069.

ABSTRACT: Several applications of Raman spectroscopy in the forensic sciences have recently been demonstrated, but few have involved the analysis of paints. Undoubtedly, this is a reflection of the sample degradation problems often encountered when a visible or near-infrared laser is focused on a light-absorbing matrix. In this study, a dispersive CCD Raman spectrometer (785 nm) was used in a configuration which collected scattered light from an excitation region 3 mm long and 80 μm wide, instead of from a focused spot. Sample degradation was not observed, and Raman spectra of automotive paints of all colors were readily obtained. Most of the paints analyzed were U.S. automobile original finishes (1974 to 1989) from the Reference Collection of Automotive Paints, and the inorganic pigments examined were those which had been identified previously by infrared spectroscopy in finishes from this collection.

Prominent peaks of rutile were observed in Raman spectra of light-colored nonmetallic finishes for both monocoats and basecoat/clearcoat systems, and the rutile peaks are readily distinguished from those of anatase. The lead chromates (Chrome Yellow, Molybdate Orange, and silica-encapsulated versions of the two) are the strongest Raman scatterers among the pigments examined, and Chrome Yellow was identified by Raman spectroscopy in several yellow and orange nonmetallic monocoats for which infrared absorptions of this pigment were not observed. Raman spectroscopy also provides an unequivocal means to distinguish Chrome Yellow from Molybdate Orange. This is particularly helpful for the analysis of paints containing light pigment loads or encapsulated pigments since the two formulations cannot be differentiated by infrared spectroscopy in such cases. The iron-containing pigments, ferric oxide, hydrous ferric oxide, and Prussian Blue, are relatively weak Raman scatterers, but peaks of hydrous ferric oxide and Prussian Blue were observed in spectra of paints containing heavy pigment loads. Because no sample preparation is required, Raman spectroscopy provides an excellent means to rapidly screen reference panels for the presence of certain pigments, and some examples of the differences in Raman spectra which occur for paints having similar colors are presented.

KEYWORDS: forensic science, criminalistics, paint analysis, automotive paint, pigment identification, Raman spectroscopy, inorganic pigments

[1] Forensic scientist, Washington State Crime Laboratory, Public Safety Building, 2nd Floor, Seattle, WA.

[2] Marketing manager, Chromex, Inc., 2705 B Pan American Freeway NE, Albuquerque, NM.

[3] Presented at the 52nd Annual Meeting of the American Academy of Forensic Sciences, February 2000, Reno, NV.

Received 20 June 2000; accepted 8 Jan. 2001.

Raman spectroscopy has considerable potential as a means to assist the forensic paint analyst in identifying some of the components of a paint, particularly when it is used in conjunction with infrared spectroscopy. Both of these spectroscopic techniques provide information about molecular vibrational transitions, but they occur by separate processes and are governed by different selection rules: for infrared absorption, a change in the dipole moment of a molecule must occur for a particular normal mode of vibration, while Raman scattering requires a change in the polarizability of a molecule. For some very symmetric molecules, there is mutual exclusivity—the transitions which are observed in infrared spectra are not observed in Raman spectra and vice versa. In general, the symmetric vibrations of a molecule, which are frequently infrared inactive or produce only weak infrared absorptions, often give rise to prominent Raman peaks. Some inorganic compounds are strong Raman scatterers because of the large changes in polarizabilities which occur for their vibrations. In certain cases where the Raman excitation energy can be absorbed by the analyte, a resonance enhancement effect might also occur for some of the vibrations associated with the chromophore of the molecule.

Because of the differences between the two methods and the wide range of Raman scattering cross sections which occur for various types of compounds, Raman data for complex mixtures may serve to help identify some components not detected by infrared spectroscopy. This may be particularly true for paints since they consist of a composite of binders, light-absorbing pigments, pigments used to produce opacity or other optical effects, and additives; with the exception of binders, these can include both inorganic and organic compounds having a wide range of concentrations.

The differences between the infrared and Raman spectra of paints are likely to be the most pronounced when certain pigments are present. Inorganic pigments may be comprised of elements or ions having a wide range of atomic numbers, which affect polarizabilities. The infrared absorptions of inorganic pigments are generally broad, whereas Raman peaks of inorganic compounds are usually narrow. Some organic pigments may have relatively large Raman scattering cross sections because they contain aromatic/highly-conjugated moieties having high molecular symmetries. When pronounced resonance enhancement effects occur for pigments, their Raman peaks might be readily observed even when the pigments are present in very low concentrations.

Despite these promising characteristics and features, only a few applications of Raman spectroscopy for forensic paint examina-

tions have been reported (1–3), although this method has been used for the analysis of several other types of evidence (4–25). This paucity undoubtedly reflects the difficulties encountered when a visible or near-infrared laser beam is focused on a light-absorbing matrix. Thermal destruction of the sample often occurs, or strong fluorescence, produced either by pigments or other paint components, may overwhelm the weaker Raman scattering peaks.

To minimize fluorescence, most of the recent Raman studies of paint have used Fourier transform (FT) Raman instruments, which use near-infrared excitation. Kuptsov (2) presented FT Raman data for some inorganic pigments and alkyds resins, but indicated that for actual paints, the method is usually limited to lighter colors (whites and yellows). Massonnet and Stoecklein (3) were able to obtain FT Raman data for some yellow, orange, and red organic pigments used in automotive paints, along with spectra of some red finishes which contain these pigments. Data for automotive paints of other colors were not presented, however, and these authors reported thermal degradation problems with blue and green phthalocyanine pigments. Massonnet and Stoecklein noted that the Raman spectra of the finishes were dominated by pigment peaks, as was observed in some other recent Raman studies involving non-automotive paints (26–31).

The intensity of Raman scattering is proportional to the fourth power of the frequency of scattered light. Consequently, FT Raman instruments, with their near-infrared lasers, require higher power levels than instruments employing visible lasers. In addition, the near-infrared detectors used with FT Raman spectrometers are less sensitive than the charge-coupled device (CCD) array detectors which are used with visible excitation instruments. The use of minimal laser power levels was particularly desirable in this study because automotive paints typically contain heavier loads of color-imparting pigments than most other types of coatings. A dispersive CCD Raman spectrometer equipped with a visible laser (785 nm) was therefore used, and this instrument was additionally operated in a collection mode which produced an excitation area consisting of a line segment rather than a focused spot. This resulted in much lower power density levels directed onto the sample surface, and Raman spectra of automotive finishes of all colors were readily obtained.

The paints examined in this study included U.S. automobile original (OEM) finishes (1974 to 1989) from the Reference Collection of Automotive Paints, more recent finishes obtained from some paint manufacturers, and paints removed from vehicles. The inorganic pigments examined were those previously identified by infrared spectroscopy in finishes from the Reference Collection of Automotive Paints (32,33). Because Raman data are complementary to infrared data, infrared spectra (4000 to 220 cm^{-1}) are also presented for the pigments and paints discussed in this work, and the features of both spectra are compared and contrasted.

Experimental

Raman Analyses

Raman spectra were acquired using a Chromex Raman 2000 spectrometer equipped with a 785 nm solid state diode laser. Rayleigh scattered radiation was removed with a thin-film dielectric edge filter, and the Stokes scattered radiation having Raman shifts between 3317 and 160 cm^{-1} was collected at a spectral bandwidth of 10 cm^{-1}. The instrument uses a single grating and the detector is a thermoelectrically cooled CCD system consisting of a 1024 by 256 array of pixels. The spectrometer is configured with both a microscope attachment and a macro sampling chamber, and the latter was used for all analyses. Two sample excitation modes, consisting of a spot focus and a line segment focus, are available. Using the macro chamber, the spot focus illuminates an area 80 μm in diameter, while the line segment focus illuminates a segment 3 mm long and 80 μm wide. The energy density (energy/area) produced by the line segment excitation is approximately 2% of the spot focus, and the line segment excitation mode was used for all analyses.

Automotive paint panels and paint chips were analyzed directly with no sample preparation by placing them horizontally in the macro chamber. Pigments powders were analyzed neat by placing them on a glass slide wrapped with aluminum foil; the powders were compressed with a second glass slide to form a flat surface. Laser power levels between 30 and 60 mW (at the sample) were used for all of the paints and pigments. Total collection times for most samples were between 10 and 60 s.

Grams32® software was used for data collection and preliminary data processing. Spectral data were then converted to JCAMP files and imported to Spectra Calc®, which was used for further mathematical processing and for preparation of data presentation formats. Currently, there is no convention regarding the direction of the abscissa scale for presentation of Raman data. All of the Raman spectra presented in this work are depicted together with infrared data, so both are shown with Raman shifts/frequencies decreasing from left to right, as is normally used for infrared data.

Infrared Analyses

Infrared spectra were acquired at a resolution of 4 cm^{-1} using an extended range (4000 to 220 cm^{-1}) Digilab FTS-7 Fourier transform infrared (FT-IR) spectrometer. Paint samples were analyzed as thin slices placed over a 1 mm diameter circular aperture in a metal disk, which was mounted in a Digilab 5X beam condenser, and 1000 scans were collected. Spectra of pigments were acquired using a low pressure diamond anvil cell (DAC) mounted in the 5X beam condenser. Pigment powders were ground with excess CsI, and this mixture was then either pressed onto a single anvil of the DAC (34,35) or pressed between both anvils. Reference spectra were obtained of CsI pressed onto the same single anvil, or pressed between both anvils, and 1000 scans were collected for both references and samples. Spectral processing functions were performed using Spectra Calc software. More details regarding the FT-IR spectrometer, the instrument parameters used for data collection, the paint and pigment sample preparation techniques, and spectral processing are presented elsewhere (33).

Automotive Paints and Pigments

Most of the paints analyzed in this study consisted of panels from the Reference Collection of Automotive Paints (Collaborative Testing Services, Inc., Herndon, Virginia); the cited colors of these paints are based on the classification system used in this collection. Both monocoats and basecoat/clearcoat finishes were examined and they will be referred to by their seven or nine character identification codes, which are described elsewhere (32,36). Panels of original finishes used on more recent vehicles were obtained from BASF, DuPont, PPG, and Mazda, while other samples were removed from salvage vehicles.

The pigments which were examined in this study included rutile, anatase, Chrome Yellow, Molybdate Orange, silica-encapsulated Molybdate Orange, diatomaceous silica, synthetic silica, ferric oxide, hydrous ferric oxide, and Prussian Blue. They are all described elsewhere (32,33).

Results and Discussion

Infrared and Raman spectra of paints containing various pigments are presented in this work, but the details of the identification of these pigments based on their infrared absorptions are presented elsewhere (32,33,37–40). Although organic pigments are not the focus of this paper, absorptions of a few of these are observed in some of the infrared spectra and their presence is noted to facilitate comparisons to Raman spectra.

Instrument Response Function and Spectral Corrections

The instrument response function of the spectrometer used in this study is depicted in Fig. 1*f*. Ideally, this function is produced by measuring the spectrum of a white light source having a constant intensity output for the spectral region of interest (for an excitation wavelength of 785 nm, the Stokes Raman shifts from 160 to 3317 cm^{-1} correspond to near-infrared radiation between 795 and 1061 nm). Such a source was not available, so the light of an incandescent lamp was used to produce Fig. 1*f*. The decrease in this function for high Raman shifts reflects the insensitivity of the CCD detector to near-infrared radiation, while the drop-off for low Raman shifts is caused by the filter system used to remove the Rayleigh line. This filter system, which is based on interference effects, also produces the sinusoidal fringes of Fig. 1*f*.

To obtain Raman spectra having relative peak intensities that are not dependent on the detection efficiency of the instrument, acquired data can be divided by the instrument response function to give normalized spectra. In the absence of a fluorescence background, this simply serves to alter the relative peak intensities. When a strong fluorescence background occurs, as observed for the paint spectrum depicted in Fig. 1*c,* fringes caused by the filter are present, which can make interpretation of data more difficult. For such cases, an instrument correction is necessary to remove the fringes and the resulting spectral contour represents the shape of the fluorescence band (which may have sharper Raman peaks superimposed on it). The normalized spectrum of Fig. 1*d,* for example, was obtained by dividing the uncorrected spectrum (Fig. 1*c*) by the instrument response function (Fig. 1*f*); the apparent rise in the baseline of this normalized spectrum above 2800 cm^{-1} is an artifact resulting from the nonlinear output of the lamp used to produce Fig. 1*f*. For the various spectra presented in this study, instrument corrections were only used when a pronounced fluorescence background was observed, and these spectra are denoted as "normalized."

Rutile

Rutile, the polymorph of titanium dioxide most often used in paints, has an infrared spectrum consisting of a very broad low frequency absorption having two shoulder features (Fig. 2*g*). In contrast, the Raman spectrum of rutile (Fig. 2*d*) has two relatively narrow peaks at 613 and 451 cm^{-1} and is easily distinguished from that of anatase (Fig. 2*e*), a second polymorph of titanium dioxide that may also be used in paints (the infrared spectrum of anatase is shown in Fig. 2*f*). Strong absorptions of rutile are observed in infrared spectra of all of the white nonmetallic monocoats in the Reference Collection of Automotive Paints (33), as illustrated by the spectrum of DC82A0466 (Fig. 2*a*), an acrylic melamine enamel. The Raman spectrum of DC82A0466 (Fig. 2*b*) is comprised primarily of rutile peaks and only very weak binder features, including three peaks at 1449, 1002, and 980 cm^{-1}, are observed. The 1002 and 980 cm^{-1} peaks have previously been assigned to ring expansion modes of the phenyl group of styrene and the triazine ring of melamine, respectively (2).

The Raman spectrum of CC77A0364, a white nonmetallic basecoat/clearcoat finish which has acrylic melamine enamel binders for both the basecoat and the clearcoat layers, is depicted in Fig. 1*c*. Other than relative increases in the weak binder peak intensities and fluorescence, results similar to those of the monocoat are obtained. It is thus evident that pigments in basecoats can be readily analyzed through clearcoats since the clearcoat layer is a weakly-scattering medium.

Lead Chromate Pigments

The two main lead chromate pigments used in automotive finishes are Chrome Yellow ($PbCrO_4 \cdot xPbSO_4$) and Molybdate Orange ($PbCrO_4 \cdot xPbMoO_4 \cdot yPbSO_4$). Both consist of solid solutions containing mostly lead chromate together with some other lead salts. Lead chromate pigments are no longer used in U.S. automobile OEM finishes, having last been used (33) in the early 1990s (and mostly phased-out in the 1980s), but they continued to be used in automotive paints in Europe (3).

Chrome Yellow—Infrared and Raman spectra of Chrome Yellow are shown in Figs. 3*f* and 3*d,* respectively. Two relatively narrow peaks at 843 and 365 cm^{-1} are observed in the Raman spectrum, together with a very weak peak at 406 cm^{-1}. Infrared and Raman spectra of a yellow nonmetallic monocoat (NN78H0476), which contains a heavy pigment load of Chrome Yellow, are depicted in Figs. 3*b* and 3*c*. As observed for white paints, the Raman spectrum of this monocoat is primarily that of the pigment; NN78H0476 has an acrylic melamine enamel binder, but the binder peaks are very weak in Fig. 3*c*.

The infrared spectrum of a second yellow nonmetallic acrylic melamine enamel monocoat, DC76H0043, is shown in Fig. 3*a*. This monocoat contains a large amount of rutile and what is likely a lead chromate pigment based on the weak broad feature at 868 cm^{-1}. The Raman spectrum of DC76H0043 (Fig. 3*e*) clearly indicates the presence of both Chrome Yellow and rutile. Moreover, the main Chrome Yellow peak at 841 cm^{-1} is nearly as intense as that of the rutile peaks, even though the infrared spectrum suggests that much more rutile than Chrome Yellow is present.

Chrome Yellow is thus a relatively strong Raman scatterer, and this pigment was identified by Raman spectroscopy in several Reference Collection of Automotive Paints yellow and orange nonmetallic monocoats for which infrared absorptions of Chrome Yellow were not observed. Raman spectroscopy is therefore particularly helpful for the analysis of paints having infrared spectra which do not provide a clear indication of whether a lead chromate pigment is present or not. The infrared spectrum of one of these paints, a yellow nonmetallic acrylic melamine enamel monocoat (74H0117), is shown in Fig. 4*c*. The weak 851 cm^{-1} peak of 74H0117 does not appear to be that of a lead chromate pigment because of its low frequency and relative sharpness, but the Raman spectrum of this finish (Fig. 4*d*) shows clearly that Chrome Yellow is present.

Molybdate Orange—Infrared and Raman spectra of Molybdate Orange are depicted in Figs. 5*a* and 5*d,* respectively. The Raman spectrum of Molybdate Orange is similar to that of Chrome Yellow (Fig. 5*h*), but the two can be distinguished based on the Raman shift of the strongest peak (826 versus 843 cm^{-1}), the 360/346 cm^{-1}

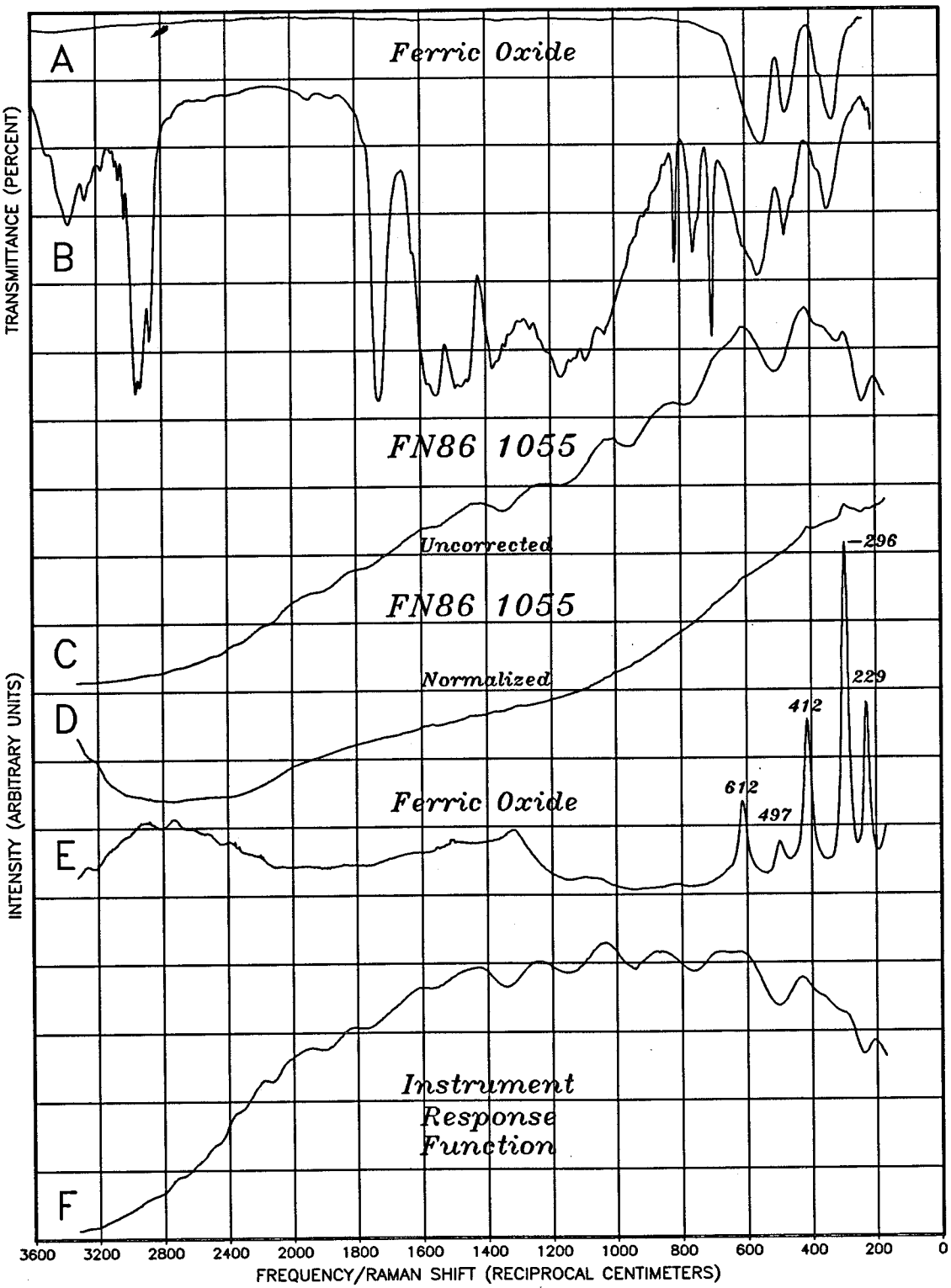

FIG. 1—(a) *Infrared spectrum of ferric oxide;* (b) *infrared spectrum of a red nonmetallic acrylic melamine enamel monocoat, FN86 1055, which contains a relatively large amount of ferric oxide;* (c) *Raman spectrum of FN86 1055, uncorrected;* (d) *normalized Raman spectrum of FN86 1055 (the spectrum of* (c) *was divided by the spectrum of* (f)*);* (e) *Raman spectrum of ferric oxide; and* (f) *Raman spectrum of a lamp used to approximate a source having a linear emission output for the range covered by the instrument.*

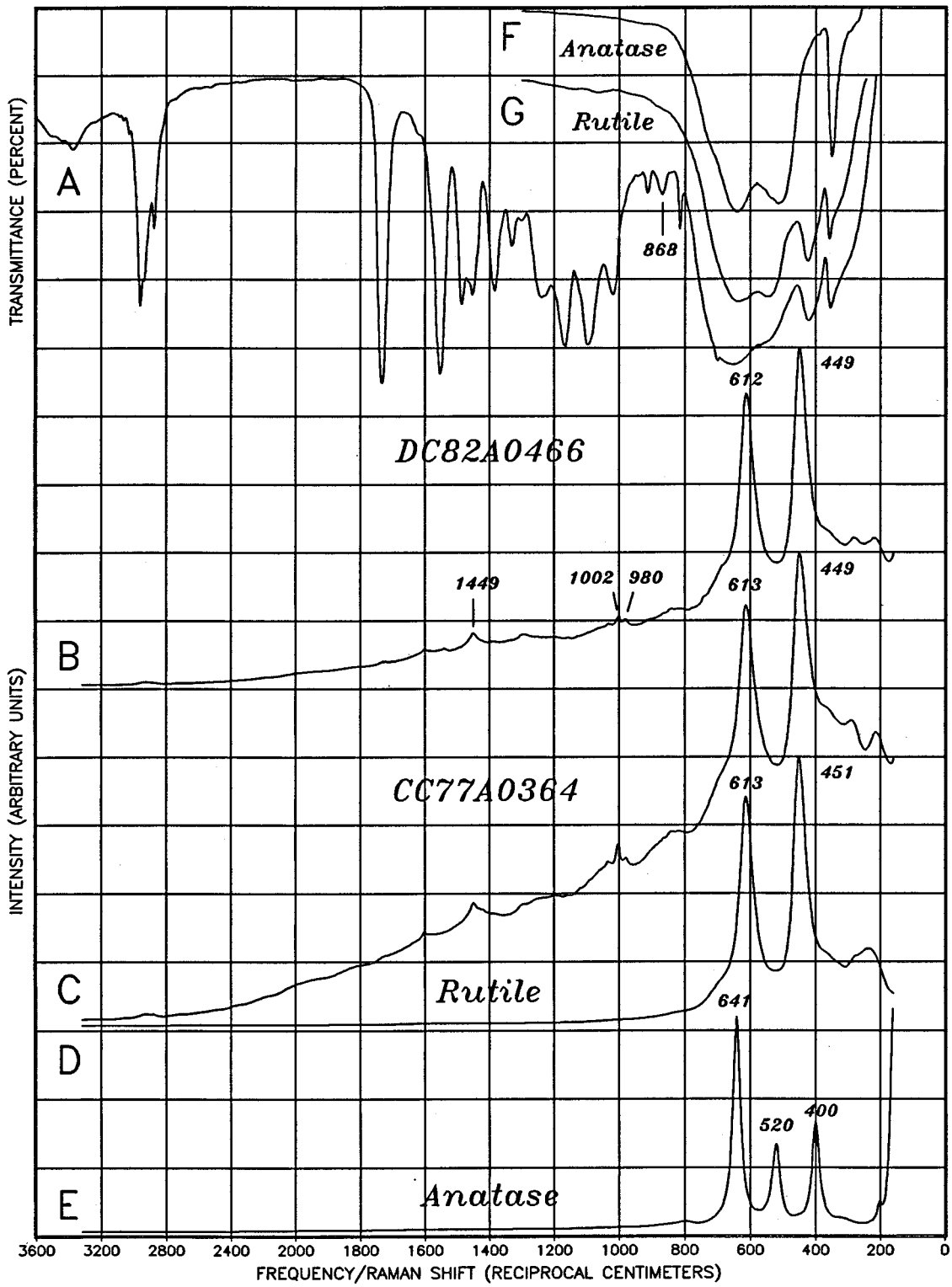

FIG. 2—(a) *Infrared spectrum of a white nonmetallic acrylic melamine enamel monocoat, DC82A0466, which contains a large amount of rutile;* (b) *Raman spectrum of DC82A0466;* (c) *Raman spectrum of CC77A0364, a white nonmetallic basecoat/clearcoat finish; both the basecoat and the clearcoat layers have acrylic melamine enamel binders and the basecoat contains a large amount of rutile;* (d) *Raman spectrum of rutile;* (e) *Raman spectrum of anatase;* (f) *infrared spectrum of anatase; and* (g) *infrared spectrum of rutile.*

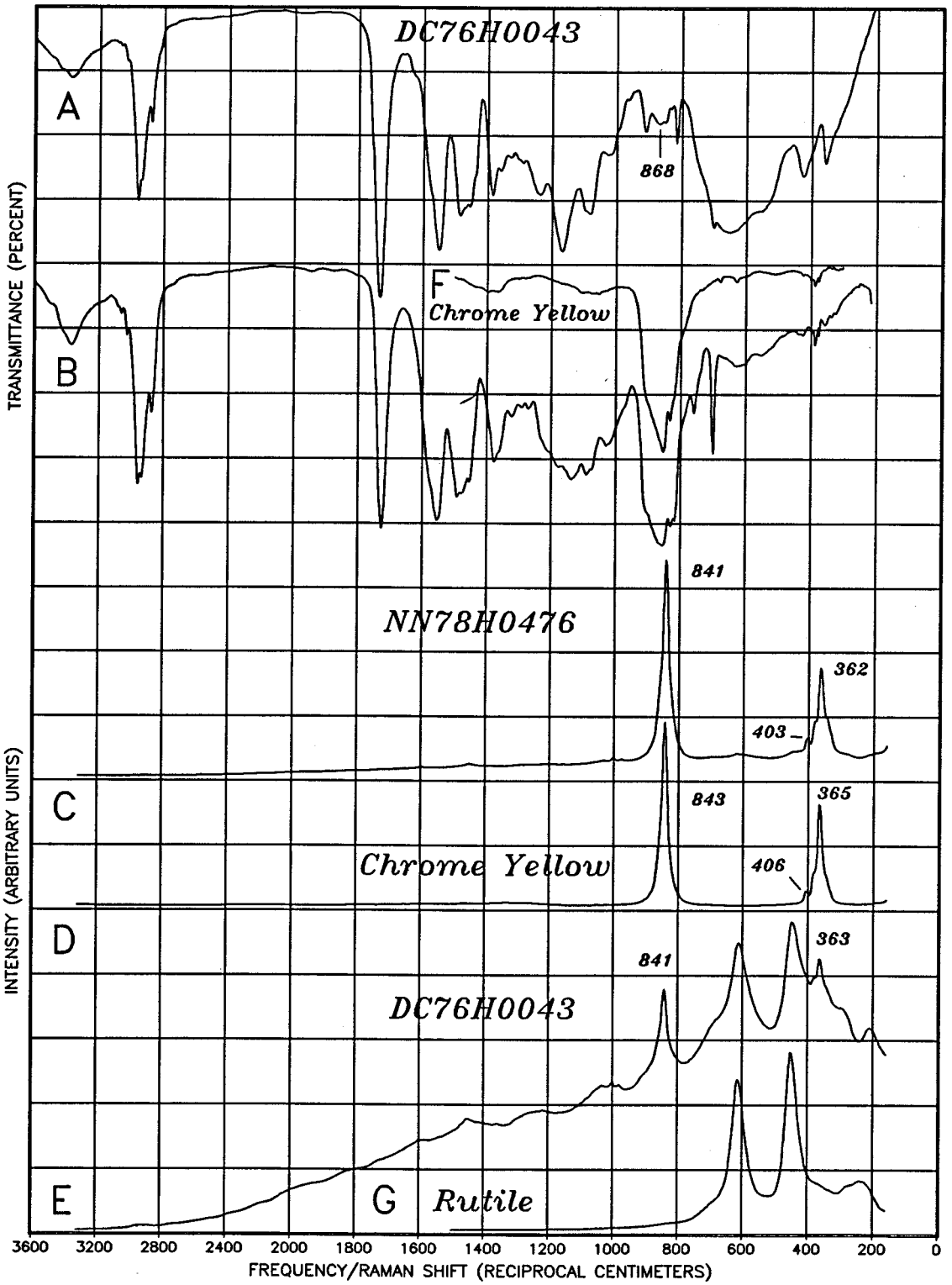

FIG. 3—(a) *Infrared spectrum of a yellow nonmetallic acrylic melamine enamel monocoat, DC76H0043, which contains a large amount of rutile and a small amount of Chrome Yellow (the Chrome Yellow absorption is marked with its frequency);* (b) *infrared spectrum of a yellow nonmetallic acrylic melamine enamel monocoat, NN78H0476, which contains a large amount of Chrome Yellow;* (c) *Raman spectrum of NN78H0476;* (d) *Raman spectrum of Chrome Yellow;* (e) *Raman spectrum of DC76H0043;* (f) *infrared spectrum of Chrome Yellow; and* (g) *Raman spectrum of rutile.*

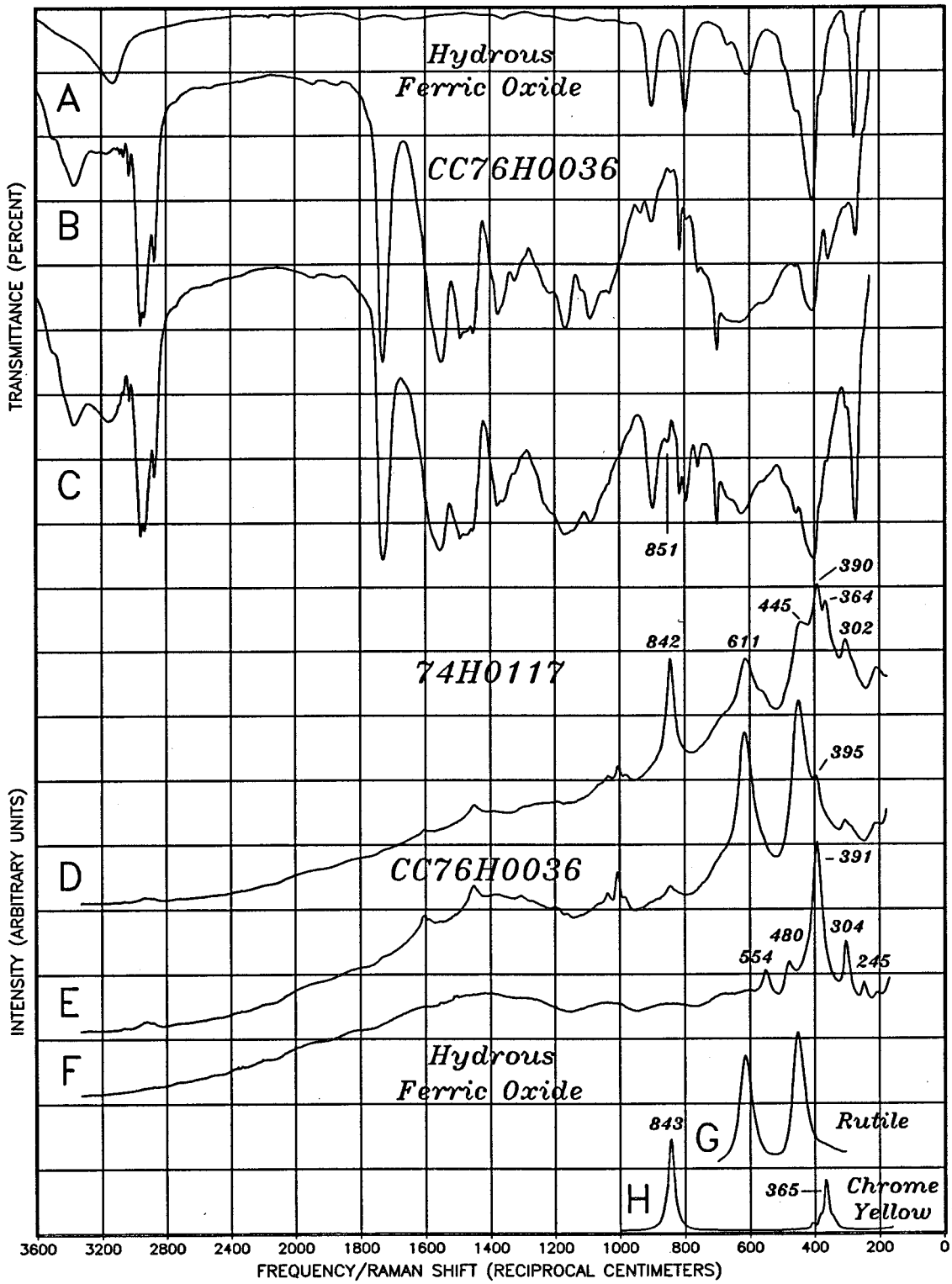

FIG. 4—(a) *Infrared spectrum of hydrous ferric oxide;* (b) *infrared spectrum of a yellow nonmetallic acrylic melamine enamel monocoat, CC76H0036, which contains large amounts of rutile and hydrous ferric oxide;* (c) *infrared spectrum of a yellow nonmetallic acrylic melamine enamel monocoat, 74H0117, which contains a large amount of hydrous ferric oxide, some rutile, and a small amount of Chrome Yellow;* (d) *Raman spectrum of 74H0117;* (e) *Raman spectrum CC76H0036;* (f) *Raman spectrum of hydrous ferric oxide;* (g) *Raman spectrum of rutile; and* (h) *Raman spectrum of Chrome Yellow.*

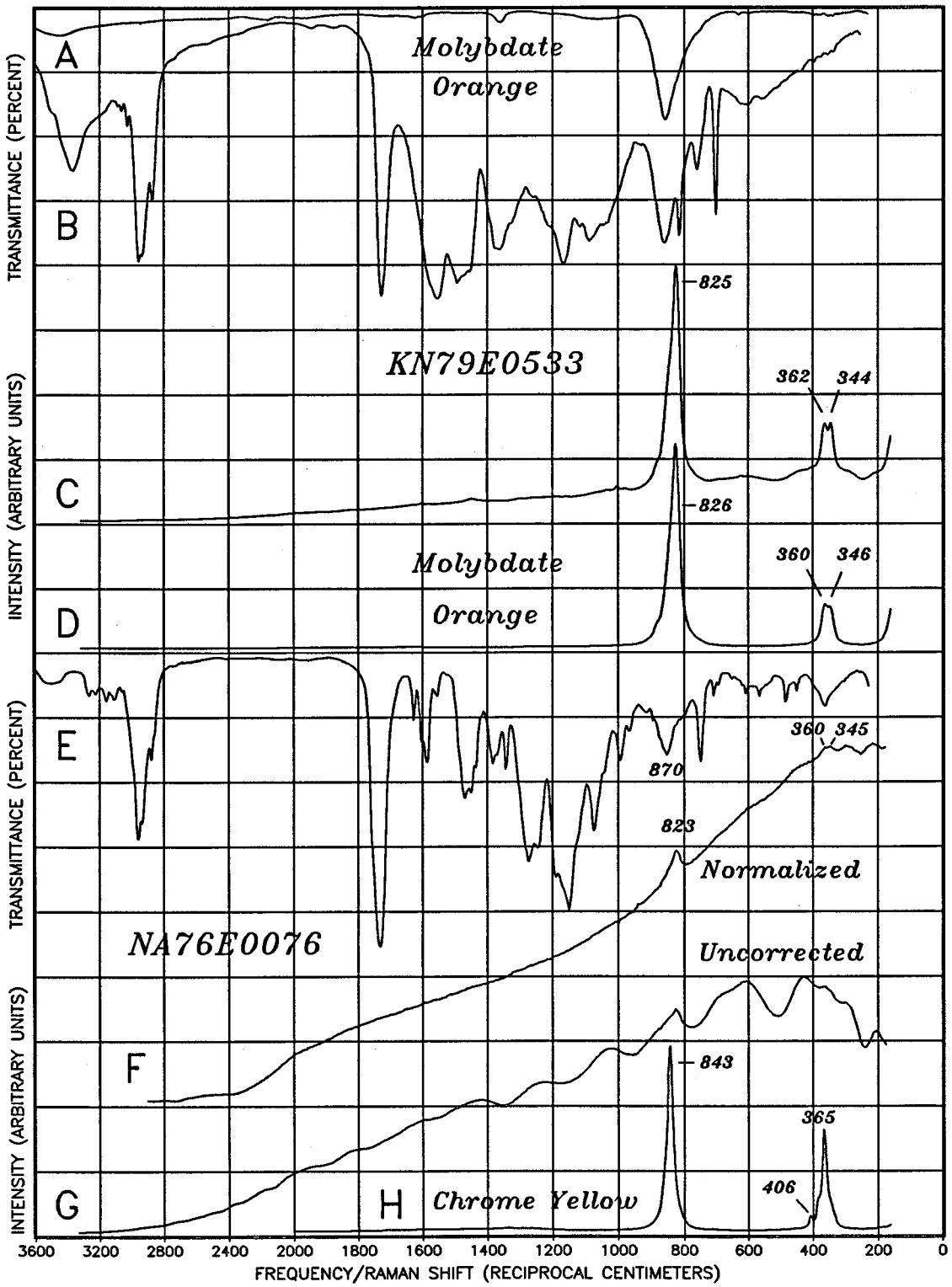

FIG. 5—(a) *Infrared spectrum of Molybdate Orange;* (b) *infrared spectrum of a red nonmetallic acrylic melamine enamel monocoat, KN79E0533, which contains a relatively large amount of Molybdate Orange;* (c) *Raman spectrum of KN79E0533;* (d) *Raman spectrum of Molybdate Orange;* (e) *infrared spectrum of a red nonmetallic acrylic lacquer monocoat, NA76E0076, which contains small amounts Molybdate Orange, Quinacridone Red Y, and ferric oxide;* (f) *normalized Raman spectrum of NA76E0076;* (g) *uncorrected Raman spectrum of NA760076; and* (h) *Raman spectrum of Chrome Yellow.*

doublet of Molybdate Orange, and the weak 406 cm^{-1} peak of Chrome Yellow.

Infrared and Raman spectra of KN79E0533, a red nonmetallic acrylic melamine enamel monocoat that contains a large amount of Molybdate Orange, are shown in Figs. 5*b* and 5*c*. As observed for the example involving a heavy pigment load of Chrome Yellow (Fig. 3*c*), the Raman spectrum of KN79E0533 is essentially that of the pigment.

The infrared spectrum of a red nonmetallic acrylic lacquer monocoat (NA76E0076), which contains small amounts of Quinacridone Red Y, ferric oxide, and a lead chromate pigment, is depicted in Fig. 5*e*. The Raman spectrum of this monocoat (Fig. 5*g*) has a strong fluorescence background, and this spectrum was normalized to give the result shown in Fig. 5*f*. Peaks of Molybdate Orange can now be seen superimposed on the fluorescence contour, and although they are weak, they can be distinguished from those of Chrome Yellow (Fig. 5*h*).

Raman spectroscopy thus provides an excellent means to differentiate between Chrome Yellow and Molybdate Orange in paints containing light pigment loads, or for paints with infrared spectra having interfering absorptions of binders or other pigments present. With light pigment loads, the infrared absorptions of Chrome Yellow and Molybdate Orange both consist of a single fairly broad indistinct feature between 870 and 855 cm^{-1} (see Figs. 3*a* and 5*e*), and the two are not easily differentiated. In contrast, the Raman spectra of such paints allow a distinction even when the observed peaks have low intensities.

Infrared spectra of some acrylic melamine enamel monocoats also have weak absorptions near 870 cm^{-1}, as observed for DC82A0466 (Fig. 2*a*), DC82E0617 (Fig. 6*b*), and NC84 0830 (Fig. 7*b*), but these are not from pigments. Lead chromate absorptions are usually broader, as observed for the spectrum of KC80E0617 (Fig. 6*a*), another monocoat which has the same color as DC82E0617. This is a subtle distinction, however, and the two absorptions can be easily confused. In contrast, the Raman spectra of KC80E0617 (Fig. 6*d*) and DC82E0617 (Fig. 6*e*) indicate clearly that the former contains Molybdate Orange and that the latter does not contain a lead chromate pigment. Note that Molybdate Orange can be identified from Fig. 6*d* even though the low frequency doublet of this pigment is partially obscured by a peak of an organic pigment.

Massonnet and Stoecklein (3) obtained a Molybdate Orange spectrum similar to Fig. 5*d* using an FT Raman instrument. These authors identified Molybdate Orange peaks in Raman spectra of 5 of 27 light red nonmetallic finishes, and 10 of 27 dark red nonmetallic finishes used on European vehicles spanning the model years 1988 to 1995. As was observed for red nonmetallic monocoats (33) used on U.S. automobiles (1974 to 1989), Molybdate Orange was also a common pigment for European vehicles. In addition, it was used for some European models manufactured after formulations involving lead-containing pigments were discontinued in the United States.

Silica-Encapsulated Lead Chromate Pigments—Some of the lead chromate pigments used in automotive paints were encapsulated with a layer of silica to minimize the possibility of a reaction between the chromates (which are oxidants) and paint binders. The infrared spectra of these pigments, such as that of silica-encapsulated Molybdate Orange (Fig. 8*a*), have strong absorptions of silica (compare Figs. 8*a* and 9*g*). Silica is a weak Raman scatterer, however, and a comparison of the Raman spectra of Molybdate Orange (Fig. 8*g*) and silica-encapsulated Molybdate Orange (Fig. 8*f*) indicates that they are virtually identical, with no apparent peaks of silica present. Some formulation information about the lead chromate pigments is thus not obtained with Raman spectroscopy, but this information can usually be deduced from infrared spectra when heavy pigment loads of encapsulated pigments are present. The absorptions of silica are quite evident, for example, in the infrared spectra of the two orange nonmetallic acrylic lacquer monocoats 74G0070 (Fig. 8*b*) and DA75G0189 (Fig. 8*c*).

Because the silica coating has little influence on the Raman spectra of the encapsulated lead chromates, this can be of benefit when interpreting data. The infrared absorptions of Chrome Yellow and Molybdate Orange in paint spectra can usually be distinguished when large quantities of the pigments are present (compare Figs. 3*f,* 3*b,* 5*a,* and 5*b*), but this is not the case for the encapsulated versions. The details of the main chromate absorption are mostly lost with encapsulation, and it is not clear, for example, which lead chromate pigment is present in DA75G0189 or 74G0070 based on their infrared spectra. The Raman spectra of DA75G0189 (Fig. 8*d*) and 74G0070 (Fig. 8*e* uncorrected, Fig. 8*h* normalized), however, clearly indicate that DA75G0189 contains (silica-encapsulated) Molybdate Orange and 74G0070 contains (silica-encapsulated) Chrome Yellow. The low Raman shift shoulders of the 840 and 363 cm^{-1} peaks of Fig. 8*e* (compare to Fig. 5*h*) further suggest that a lesser amount of Molybdate Orange may also present in 74G0070 (which is not unexpected for this orange paint since Molybdate Orange has a very red shade). This can be confirmed using elemental analysis, but such detailed pigment formulation information cannot be easily deduced from the broad chromate infrared absorption.

High Resolution Data—Chrome Yellow, Molybdate Orange, and some monocoats which contain heavy pigment loads of the two pigments were also analyzed using a higher spectral resolution (this was not used for routine analysis since this limits the spectral range of the instrument). The range of the instrument was also adjusted to allow the collection of data having lower Raman shifts. For resolutions of approximately 4 cm^{-1} or higher, the Chrome Yellow 365 cm^{-1} peak (Fig. 5*h*) was resolved into a main peak at 359 cm^{-1} with satellite peaks at 328, 339, and 377 cm^{-1}, and a lower Raman shift peak at 135 cm^{-1} was observed. For Molybdate Orange (Fig. 5*d*), a shoulder peak at 377 cm^{-1} was resolved and a lower Raman shift peak at 151 cm^{-1} was seen. The resolved pigment features were also observed in spectra of the monocoats. When high laser power levels were used, the Molybdate Orange 360/346 cm^{-1} doublet (377/360/346 cm^{-1} for higher resolutions) coalesced into a single unresolved band, and this was observed for spectra of both the neat pigment and monocoats containing various levels of the pigment. This likely arises from laser heating, as this effect generally causes band broadening in Raman spectra (41).

Diatomaceous Silica and Synthetic Silica

The use of large amounts of silica in automotive paints is much more common for undercoats (42) than for finish layers, but diatomaceous silica and synthetic silica were identified in a few U.S. automobile (1974 to 1989) OEM black nonmetallic monocoats (33). The two were used as flatting agents in these particular paints, which have semigloss or eggshell finishes. Infrared spectra of two of these monocoats, DC83 1031 and KC83 1031, are presented in Figs. 9*b* and 9*h,* respectively. DC83 1031 contains diatomaceous silica (Fig. 9*a*) and KC83 1031 contains synthetic silica (Fig. 9*g*).

The Raman spectra of DC83 1031 and KC83 1031 are shown in Figs. 9*c* and 9*e,* respectively, together with Raman spectra of diatomaceous silica (Fig. 9*d*) and synthetic silica (Fig. 9*f*). As noted,

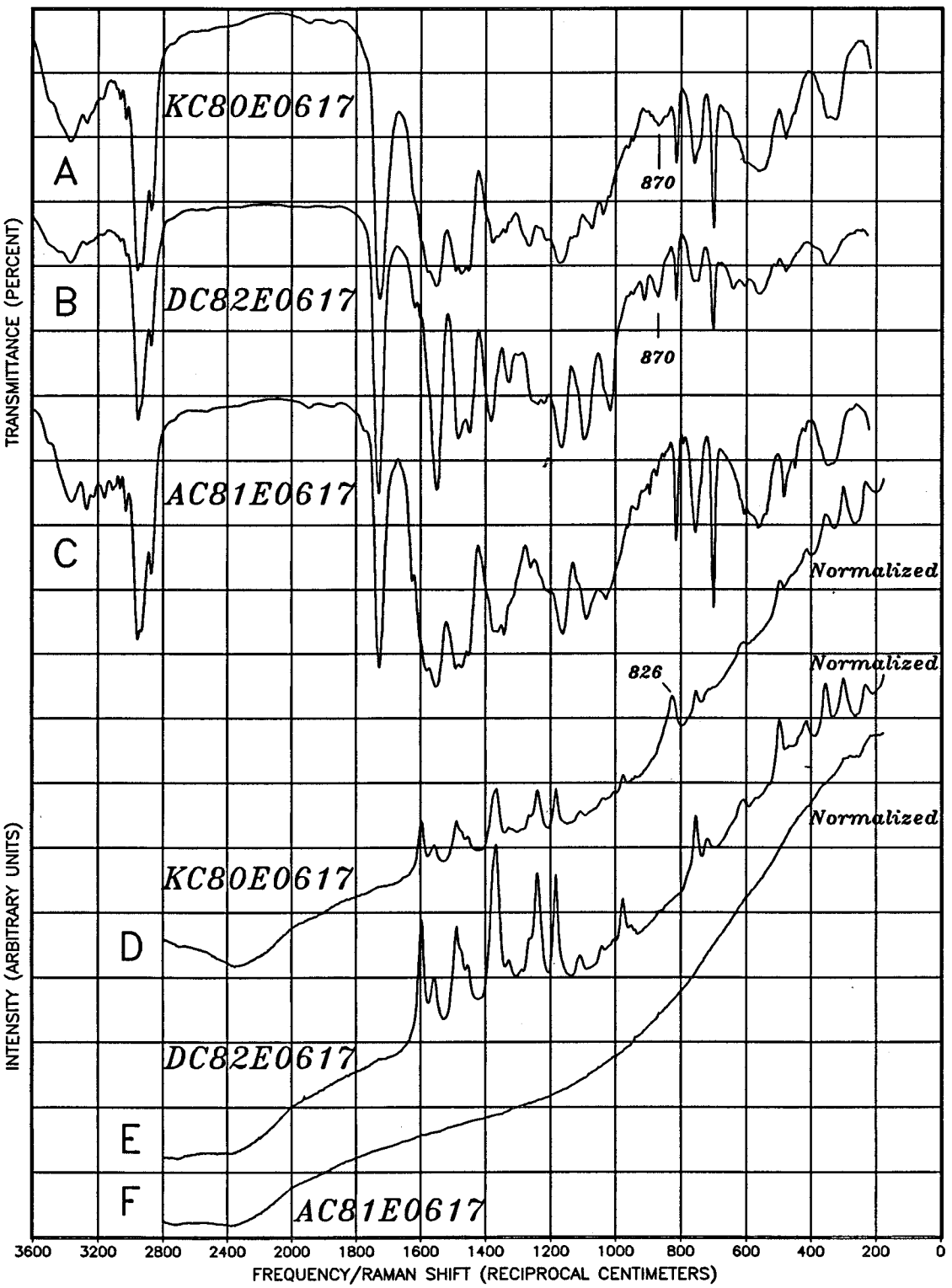

FIG. 6—*Infrared spectra of three red nonmetallic acrylic melamine enamel monocoats of Reference Collection of Automotive Paints color 0617:* (a) *KC80E0617;* (b) *DC82E0617; and* (c) *AC81E0617; all three monocoats contain ferric oxide, and KC80E0617 and AC81E0617 also contain small amounts of Molybdate Orange and Quinacridone Violet, respectively. Normalized Raman spectra of the three monocoats:* (d) *KC80E0617;* (e) *DC82E0617; and* (f) *AC81E0617.*

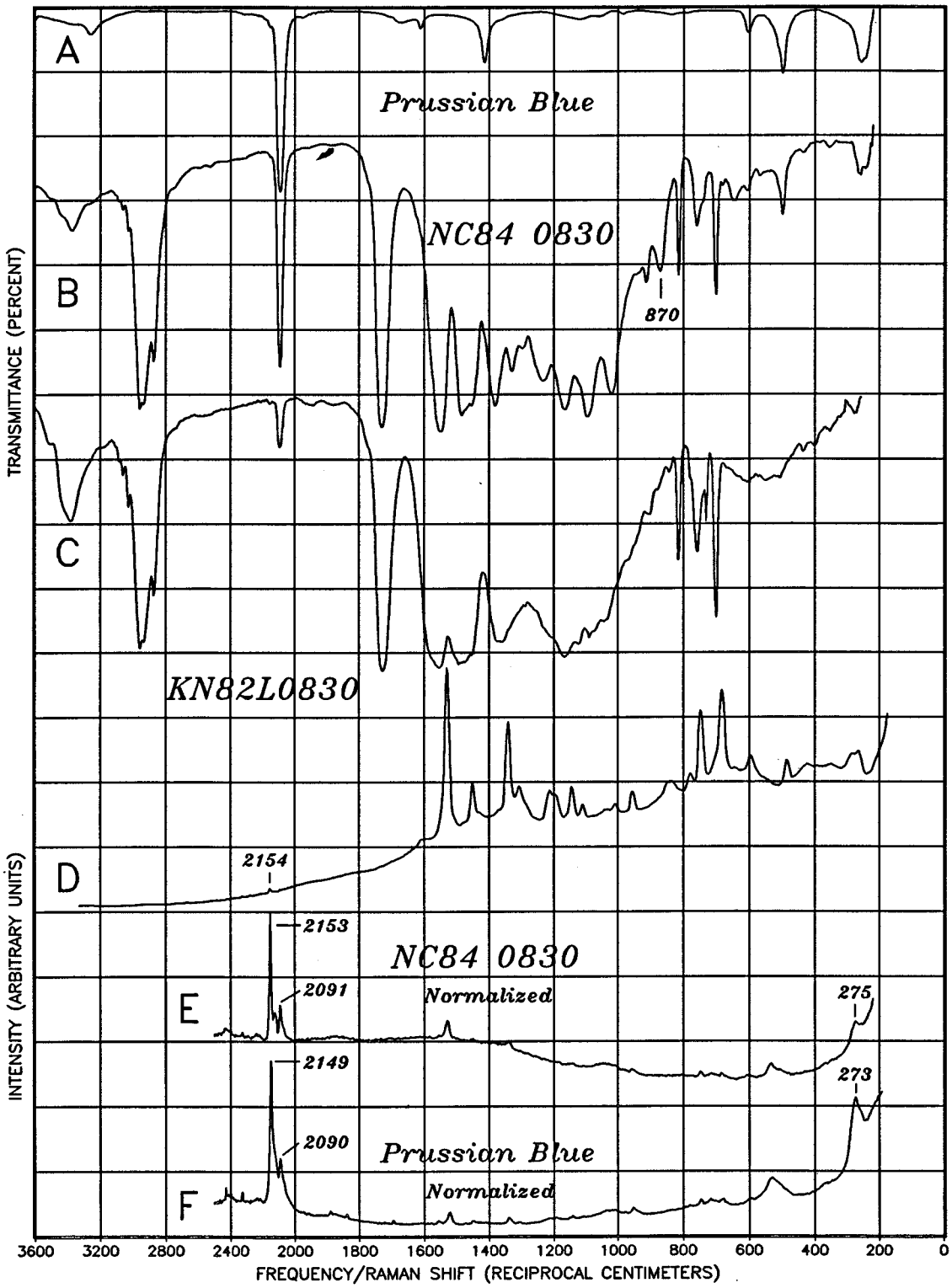

FIG. 7—(a) *Infrared spectrum of Prussian Blue;* (b) *infrared spectrum of a dark blue nonmetallic acrylic melamine enamel monocoat, NC84 0830, which contains a large amount of Prussian Blue;* (c) *infrared spectrum of a dark blue nonmetallic acrylic melamine enamel monocoat, KN82L0830, which contains a small amount of Prussian Blue; this monocoat has the same Reference Collection of Automotive Paints color as NC84 0830;* (d) *Raman spectrum of KN82L0830;* (e) *normalized Raman spectrum of NC84 0830; and* (f) *normalized Raman spectrum of Prussian Blue.*

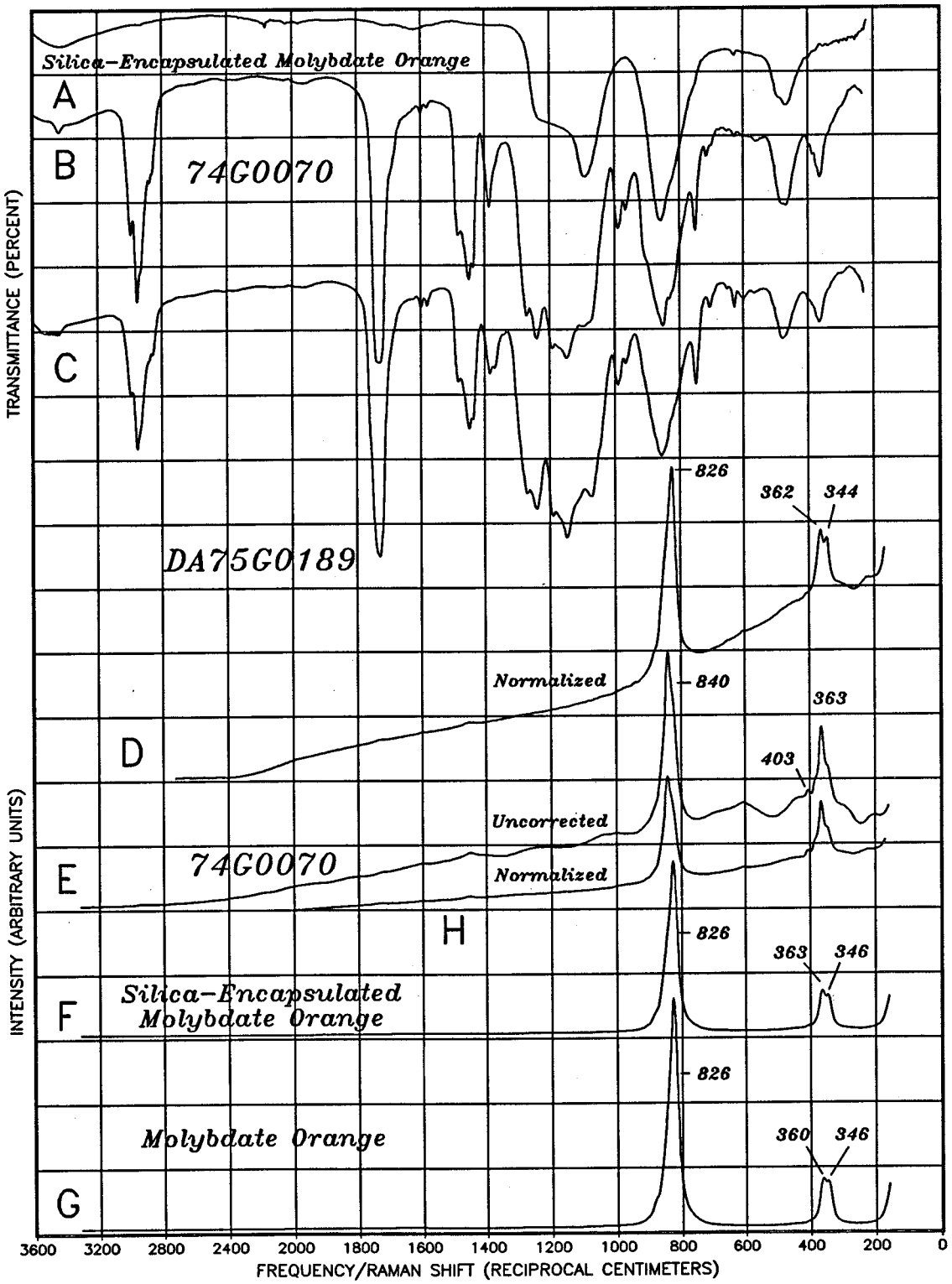

FIG. 8—(a) *Infrared spectrum of silica-encapsulated Molybdate Orange;* (b) *infrared spectrum of an orange nonmetallic acrylic lacquer monocoat, 74G0070, which contains a large amount of silica-encapsulated Chrome Yellow; silica-encapsulated Molybdate Orange is likely also present;* (c) *infrared spectrum of a second orange nonmetallic acrylic lacquer monocoat, DA75G0189, which contains a large amount of silica-encapsulated Molybdate Orange;* (d) *normalized Raman spectrum of DA75G0189;* (e) *uncorrected Raman spectrum of 74G0070;* (f) *Raman spectrum of silica-encapsulated Molybdate Orange;* (g) *Raman spectrum of Molybdate Orange; and* (h) *normalized Raman spectrum of 74G0070.*

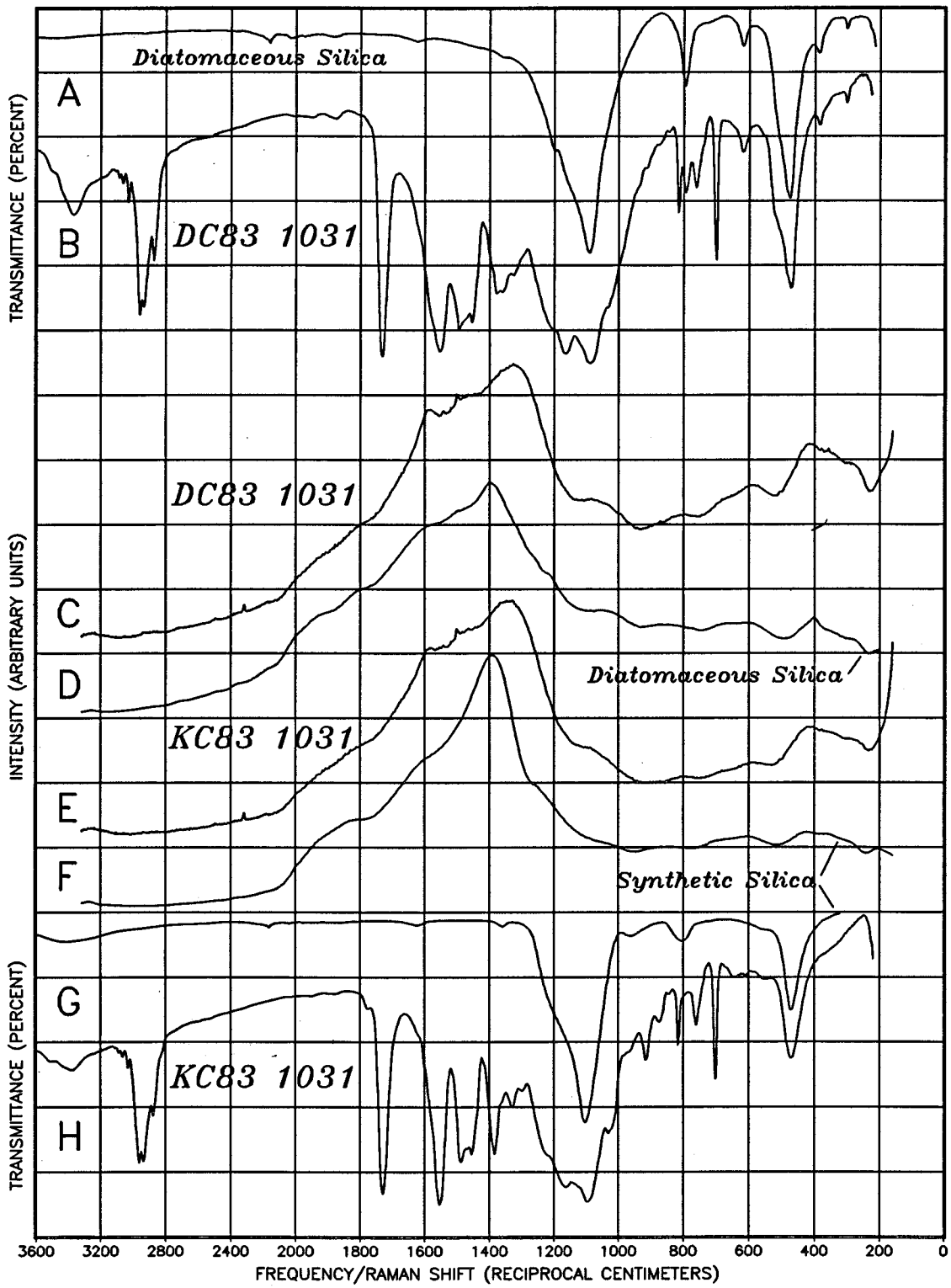

FIG. 9—(a) *Infrared spectrum of diatomaceous silica;* (b) *infrared spectrum of a black nonmetallic acrylic melamine enamel monocoat, DC83 1031, which contains diatomaceous silica;* (c) *Raman spectrum of DC83 1031;* (d) *Raman spectrum of diatomaceous silica;* (e) *Raman spectrum of KC83 1031, a black nonmetallic acrylic melamine enamel monocoat which contains synthetic silica;* (f) *Raman spectrum of synthetic silica;* (g) *infrared spectrum of synthetic silica; and* (h) *infrared spectrum of KC83 1031.*

silica is a weak Raman scatterer (which is one of the reasons objects in glass containers can often be analyzed intact using Raman spectroscopy), and all four spectra consist primarily of the broad fluorescence band of silica. The very weak sharp peaks at 2320 cm^{-1} in the spectra of the paints (Figs. 9*c* and 9*e*) are from atmospheric nitrogen; they appear in these particular spectra because longer collection times (1000 sec) were used. Because the silica pigments are such weak Raman scatterers, infrared spectroscopy is clearly the method of choice when considering vibrational spectroscopic techniques to identify these extender pigments.

Iron-Containing Pigments

Three iron-containing pigments, ferric oxide (Fe_2O_3), hydrous ferric oxide ($FeO{\cdot}OH$), and Prussian Blue ($Fe_4[Fe(CN)_6]_3$), may be found in automotive paints. For U.S. automobile (1974 to 1989) OEM monocoats, ferric oxide (rust colored), and hydrous ferric oxide (yellow) were very common pigments used in nonmetallic and metallic finishes having a wide range of colors (33), while Prussian Blue was used primarily to create a dark blue shade in some nonmetallic finishes (32). Ferric oxide and hydrous ferric oxide continue to be widely used in automotive paints. Formulations involving Prussian Blue have been mostly discontinued for U.S. automobile OEM finishes, although they are still used for refinishes (personal communication, DuPont Automotive Products, July 1999). The iron-containing pigments are relatively weak Raman scatterers, although they are stronger scatterers than the silica pigments.

Ferric Oxide—Infrared spectra of ferric oxide and FN86 1055, a red nonmetallic acrylic melamine enamel monocoat that contains a relatively large amount of this pigment, are depicted in Figs. 1*a* and 1*b,* respectively. Raman spectra of ferric oxide and FN86 1055 (normalized data) are shown in Figs. 1*e* and 1*d.* The Raman spectrum of this pigment has more peaks than the infrared spectrum, but these are not likely to be observed for most paints. Two ferric oxide Raman peaks are seen as weak or very weak features superimposed on the fluorescence contour of Fig. 1*d,* and two more can be detected only with very close scrutiny. The monocoat (FN86 1055) chosen for this example has stronger infrared absorptions of ferric oxide than most of the other finishes in which this pigment was identified, so Raman spectroscopy (employing the excitation conditions used in this study, at least) is not likely to be useful for the identification of ferric oxide in most automotive paints.

Hydrous Ferric Oxide—Infrared and Raman spectra of hydrous ferric oxide are shown in Figs. 4*a* and 4*f,* respectively, while similar data for 74H0117, a yellow nonmetallic acrylic melamine enamel monocoat that contains a heavy load of this pigment, are shown in Figs. 4*c* and 4*d.* The two strongest Raman peaks of hydrous ferric oxide are observed at 390 and 302 cm^{-1} in Fig. 4*d,* and the weaker 554 cm^{-1} feature occurs as a shoulder to a rutile 611 cm^{-1} peak. The second rutile peak is observed at 445 cm^{-1}, and two peaks of Chrome Yellow occur at 842 and 364 cm^{-1}.

A comparison of the infrared and Raman spectra of 74H0117 illustrates the effects of differences in the relative infrared absorption coefficients of hydrous ferric oxide, rutile, and Chrome Yellow versus differences in their relative Raman scattering cross sections. The low frequency region of the infrared spectrum of this monocoat is dominated by very strong absorptions of hydrous ferric oxide (Fig. 4*a*), and the broad dipping background on which these features appear strongly suggest that rutile absorptions are also present. As noted, it is questionable whether the 851 cm^{-1} peak is due to Chrome Yellow, but in any case, it is a weak feature. The Raman spectrum of 74H0117 (Fig. 4*d*) indicates the unmistakable presence of both rutile and Chrome Yellow along with hydrous ferric oxide, and the intensities of the main Raman peaks of all three pigments are comparable. Clearly, a more revealing and definitive picture of the pigment composition of this particular paint is obtained by considering both infrared and Raman data.

The infrared spectrum of another yellow nonmetallic acrylic melamine enamel monocoat (CC76H0036) that has strong absorptions of both rutile and hydrous ferric oxide is shown in Fig. 4*b.* The Raman spectrum of CC76H0036 (Fig. 4*e*) consists primarily of rutile peaks, with the main hydrous ferric oxide peak manifested as a weaker shoulder peak at 395 cm^{-1}. Note that binder peaks are relatively strong in this spectrum.

Prussian Blue—The cyano C≡N stretching fundamental near 2100 cm^{-1} is the most conspicuous feature of the infrared spectrum of Prussian Blue (Fig. 7*a*), and of spectra of many paints which contain this pigment (Figs. 7*b* and 7*c*). The Raman spectrum of Prussian Blue (Fig. 7*f*) includes cyano peaks at 2149 and 2090 cm^{-1} together with a low Raman shift peak at 273 cm^{-1}, but Prussian Blue is a relatively weak Raman scatterer (evidenced, for example, by the presence of the 2320 cm^{-1} atmospheric nitrogen peak of Fig. 7*f*). At higher laser power levels, a very broad fluorescence band is also observed (centered near 1400 cm^{-1}) for both the pigment and monocoats containing heavy pigment loads of Prussian Blue, suggesting that this feature may arise from a photo- or thermal-decomposition product of the pigment.

Infrared and Raman spectra of NC84 0830, a dark blue nonmetallic acrylic melamine enamel monocoat that contains a large amount of Prussian Blue, are shown in Figs. 7*b* and 7*e,* respectively. The three Prussian Blue pigment peaks can be seen in the Raman spectrum. Infrared and Raman spectra of a second dark blue nonmetallic acrylic melamine enamel monocoat (KN82L0830) that contains a lesser amount of Prussian Blue are shown in Figs. 7*c* and 7*d.* The cyano stretching absorption is readily observed in the infrared spectrum of this monocoat, but the cyano Raman peak at 2154 cm^{-1} is quite weak. Raman spectroscopy can thus serve to corroborate the presence of Prussian Blue in some paints, but low levels of this pigment are more easily detected using infrared spectroscopy.

Relative Raman Scattering Cross Sections of Inorganic Pigments

The relative Raman scattering cross sections of the pigments examined in this study were gaged using several criteria, including: the peak intensities of spectra of neat pigment powders collected for similar time periods; the pigment peak intensities observed for spectra of paints containing various concentrations of a particular pigment; and the relative pigment peak intensities observed for spectra of paints containing various combinations of two or more pigments of interest; infrared spectra of these same paints were used to provide some measure of the relative amounts of pigments present.

From these comparisons, it was evident that the lead chromate pigments—and Chrome Yellow in particular—are the strongest Raman scatterers among the inorganic pigments examined, followed by (in order of decreasing scattering strengths) rutile, the iron-containing pigments, and silica. The scattering efficiencies of the pigments, however, seem to be quite dependent on the color of the finish in which they occur. This most likely reflects differences in the penetration depth of the exciting laser beam for paints of various colors. Chrome Yellow and Molybdate Orange, for example, have similar chemical compositions and one might reasonably ex-

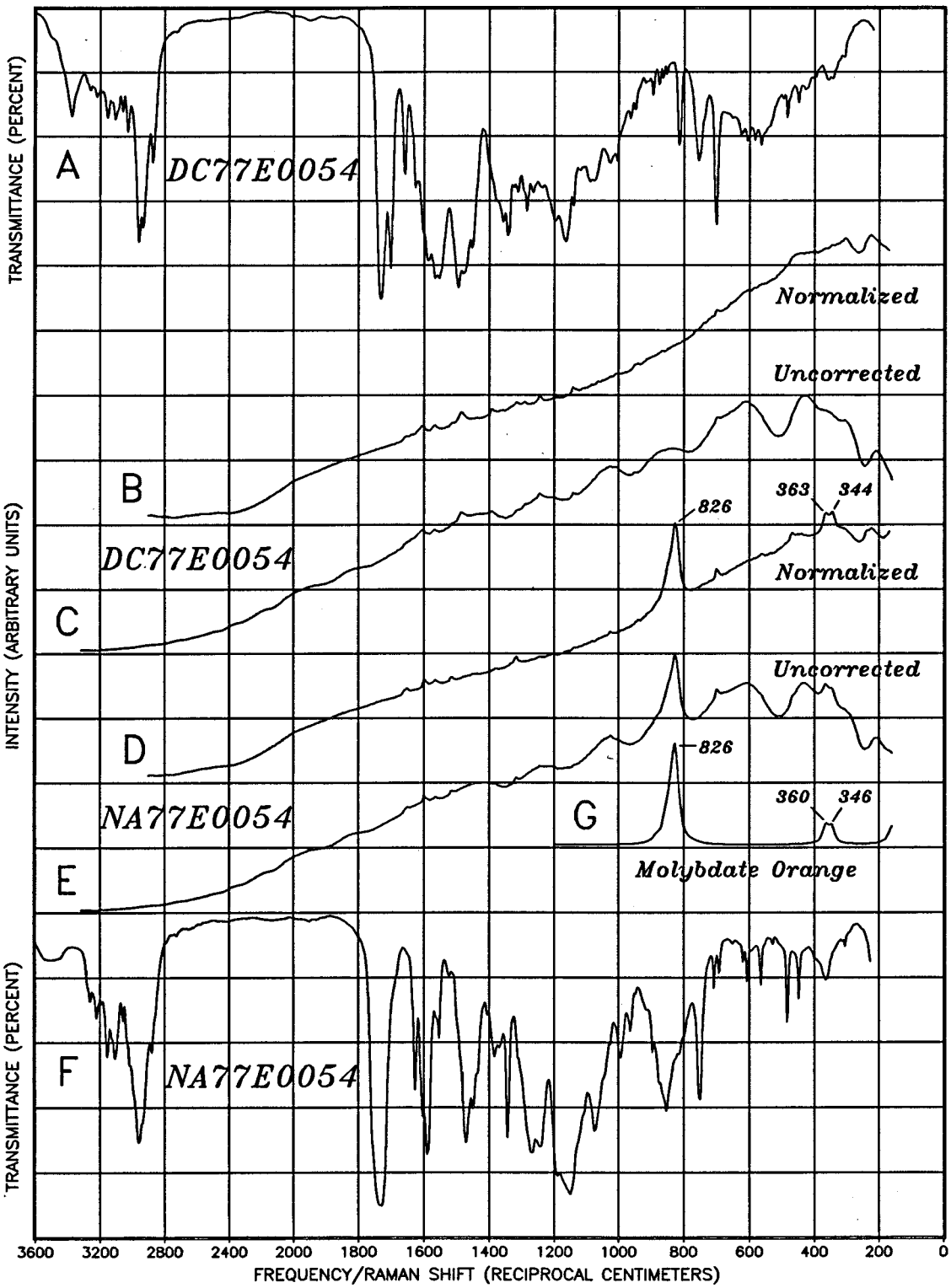

FIG. 10—(a) *Infrared spectrum of a red nonmetallic acrylic melamine enamel monocoat, DC77E0054, which contains Quinacridone Red Y, Benzimidazolone Orange, ferric oxide, and rutile;* (b) *normalized Raman spectrum of DC77E0054;* (c) *uncorrected Raman spectrum of DC77E0054;* (d) *normalized Raman spectrum of a red nonmetallic acrylic lacquer monocoat, NA77E0054, which contains Quinacridone Red Y and Molybdate Orange; this monocoat has the same Reference Collection of Automotive Paints color as DC77E0054;* (e) *uncorrected Raman spectrum of NA77E0054;* (f) *infrared spectrum of NA77E0054; and* (g) *Raman spectrum of Molybdate Orange.*

pect them to have comparable Raman scattering cross-sections, but Chrome Yellow is clearly a stronger scatterer. The 785 nm laser light would be expected to penetrate deeper into yellow paints compared to red ones, since the absorption maxima of the red samples are closer to the laser wavelength. Consequently, the effective sampling volume would be greater for yellow samples compared to those having red colors, and more scattered light can be collected (Molybdate Orange, despite its name, is actually much more common in red finishes (33) than orange ones).

Another example of this effect involves rutile, which unlike the other pigments, is not colored. Infrared and Raman spectra of DC77E0054, a red nonmetallic monocoat which contains a moderate amount of rutile, are depicted in Figs. 10*a* and 10*b,* respectively. The rutile peaks are barely noticeable in the Raman spectrum of this paint, even though such peaks are usually readily observed in spectra of yellow paints which contain comparable amounts of this pigment (all white automotive finishes contain much more rutile so they are not as useful for comparison).

Screening of Reference Panels

Because intact paint samples can be analyzed directly with no sample preparation using Raman spectroscopy, this method provides an excellent means to screen reference paint panels to determine if certain pigments are present. This can be helpful when attempting to identify an unknown finish that is compared to various reference panels, or when generating a database of pigment compositions involving a large number of samples. The presence of pigments in both monocoats and basecoat layers of basecoat/clearcoat finishes can be determined by this method.

The color and type of finish (nonmetallic or metallic) of an automotive paint are among its most distinctive and easily-determined characteristics (43,44). A screening process intended to help identify an unknown paint would thus normally be used to differentiate between reference panels having similar colors. Examples of some of the differences that occur in Raman spectra of monocoats of three Reference Collection of Automotive Paints colors are therefore presented.

Raman spectra (uncorrected and normalized) of two red nonmetallic monocoats of color 0054 are shown in Figs. 10*b* to 10*e.* NA77E0054 (Fig. 10*d*) contains Molybdate Orange (Fig. 10*g*), and the peaks of this pigment are easily seen in the uncorrected spectrum as well (Fig. 10*e*); DC77E0054 (Fig. 10*b*) does not contain a lead chromate pigment. Infrared spectra of DC77E0054 and NA77E0054 are shown in Figs. 10*a* and 10*f,* respectively. DC77E0054 contains Benzimidazolone Orange, Quinacridone Red Y, ferric oxide, and rutile, while NA77E0054 contains Quinacridone Red Y and a lead chromate pigment (which, as discussed, cannot be easily identified by infrared spectroscopy when present in small quantities). As mentioned, only very weak rutile peaks are observed in the Raman spectrum of DC77E0054 (Fig. 10*b*), together with very weak peaks of an organic pigment.

Raman spectra of two dark blue nonmetallic monocoats of color 0830, KN82L0830 and NC84 0830, are depicted in Figs. 7*d* and 7*e,* respectively. As noted previously, both contain Prussian Blue, but at different levels, and the Raman spectra of the two paints suggest that this is probably also the case. More significantly for screening purposes, however, the spectrum of KN82L0830 (Fig. 7*d*) contains strong peaks of an organic pigment that clearly distinguishes the two paints.

Raman spectra of three red nonmetallic monocoats of color 0617 are shown in Figs. 6*d* to 6*f.* As noted, KC80E0617 (Fig. 6*d*) contains Molybdate Orange but DC82E0617 (Fig. 6*e*) and AC81E0617 (Fig. 6*f*) do not. The infrared spectra of the monocoats (Figs. 6*a* to 6*c*) indicate that all three contain ferric oxide, and the Raman spectrum of AC81E0617 (Fig. 6*f*) appears to contain two very weak peaks of this pigment near 300 and 230 cm^{-1} (see Fig. 1*e*). The infrared spectrum of AC81E0617 (Fig. 6*c*) also has weak peaks of Quinacridone Violet, but its Raman spectrum (Fig. 6*f*) has little indication of the presence of organic pigment peaks. The Raman spectra of KC80E0617 (Fig. 6*d*) and DC82E0617 (Fig. 6*e*), in contrast, have prominent peaks of an (unidentified) organic pigment.

Even without a knowledge of which specific organic pigments are responsible for producing the Raman peaks of Figs. 6*d,* 6*e,* and 7*d,* these spectral features can still be used to help differentiate paints having similar colors. These particular Raman spectra are especially noteworthy, however, since the corresponding infrared spectra (Figs. 6*a,* 6*b,* and 7*c,* respectively) lack significant absorptions of organic pigments. These Raman peaks can thus be used to identify some organic pigments that are present in concentrations too low to be determined by infrared spectroscopy, and this topic will be explored further in subsequent papers in this series.

A Note of Caution

During one prolonged analysis of Prussian Blue using relatively high laser power levels (more than 100 mW at the sample), the neat powder, which has a dark blue hue, ignited. This was not realized until after the sample chamber was opened, at which time considerable smoke was observed and most of the pigment had developed a crusty rust-colored surface. The reaction continued after the sample was removed from the instrument and the heat generated from it caused the glass slide, on which the sample was situated, to crack. Fortunately, the reaction of this pigment ($Fe_4[Fe(CN)_6]_3$) did not appear to involve the generation of hydrogen cyanide, but clearly this incident indicates the need for caution when certain samples are subjected to analysis using a laser (which in this case had a very diffuse focus).

In their study of explosives and propellants using an FT Raman instrument, McNesby et al. (15) noted that M30, a dark gray product which contains 40% nitroguanidine, 28% nitrocellulose, and 22% nitroglycerin, also combusted during analysis. A 1.06 μm Nd:YAG laser was used with 400 mW of power at the sample, and the M30 ignited after a few seconds of exposure to the laser light. Lewis et al., in their study of explosives using various Raman instruments (18), reported that HNS-II, a product which contains 2,2′, 4,4′,6,6′-hexanitrostilbene, readily burned when exposed to 50 mW of laser power (these authors did not indicate, however, whether this product was colored or not). None of the other materials examined by either McNesby et al. or Lewis et al. was cited as producing such problems.

Acknowledgments

The authors would like to thank: Cookson Pigments Inc., Degussa Corp., DuPont White Pigment and Mineral Products, Farwest Paint Manufacturing Co., Heubach Inc., and Wayne Pigment Corp. for providing samples and information; DuPont Automotive Products for providing information; and Ms. Chesterene Cwiklik (Cwiklik & Associates), Ms. Ingrid Dearmore (WSCL), Dr. Bill Gresham (WSCL), Ms. Cynthia Graff (WSCL), Ms. Helen Griffin (WSCL), Ms. Becky Huff (FBI Laboratory), and Ms. Marianne Stam (California Department of Justice Forensic Science Laboratory, Riverside) for taking the time to review this manuscript. One of the authors would also like to thank a descendant of the "Head of the Cararra Marble Mines" family of Italy, for allowing this FTIRUser to become a RamanUser once again.

References

1. Guineau B. Microanalysis of painted manuscripts and colored archeological materials by Raman laser microprobe. J Forensic Sci 1984;29: 471–85.
2. Kuptsov AH. Applications of Fourier transform Raman spectroscopy in forensic science. J Forensic Sci 1994;39:305–18.
3. Massonnet G, Stoecklein W. Identification of organic pigments in coatings: applications to red automotive topcoats. Part III: Raman spectroscopy (NIR FT-Raman). Sci and Justice 1999;39:181–7.
4. Carver FWS, Sinclair TJ. Spectroscopic studies of explosives. 1. Detection of nitro compounds on silica gel and carbon by non-resonant Raman spectroscopy. J Raman Spectrosc 1983;14:410–4.
5. Lang PL, Katon JE, O'Keefe JF, Schiering DW. The identification of fibers by infrared and Raman microspectroscopy. Microchem J 1986; 34:319–31.
6. Hodges CM, Hendra PJ, Willis HA, Farley T. Fourier transform Raman spectroscopy of illicit drugs. J Raman Spectrosc 1989;20:745–9.
7. Bourgeois D, Church SP. Studies of dyestuffs by Fourier transform Raman spectroscopy. Spectrochim Acta 1990;46A:295–301.
8. Hodges CM, Akhavan J. The use of Fourier transform Raman spectroscopy in the forensic identification of illicit drugs and explosives. Spectrochim Acta 1990;46A:303–7.
9. Hendra PJ, Maddams WF, Royaud IAM, Willis HA, Zichy V. The application of Fourier transform Raman spectroscopy to the identification and characterization of polyamides—I. Single number nylons. Spectrochim Acta 1990;46A:747–56.
10. Maddams WF, Royaud IAM. The application of Fourier transform Raman spectroscopy to the identification and characterization of polyamides—II. Double number nylons. Spectrochim Acta 1990;46A: 1327–33.
11. Neville GA, Shurvell HF. Fourier transform Raman and infrared vibrational study of diazepam and four closely related 1,4-benzodiazepines. J Raman Spectrosc 1990;21:9–19.
12. Akhavan J. Analysis of high-explosive samples by Fourier transform Raman spectroscopy. Spectrochim Acta 1991;47A:1247–50.
13. By A, Neville GA, Shurvell HF. Fourier transform infrared/Raman differentiation and characterization of *cis*- and *trans*- 2,5-dimethoxy-4, β-dimethyl-β-nitrostyrenes: precursors to the street drug STP. J Forensic Sci 1992;37:503–12.
14. Bouffard SP, Sommer AJ, Katon JE, Godber S. Use of molecular microspectroscopy to characterize pigment-loaded polypropylene single fibers. Appl Spectrosc 1994;48:1387–93.
15. McNesby KL, Wolfe JE, Morris JB, Pesce-Rodriguez RA. Fourier transform Raman spectroscopy of some energetic materials and propellant formulations. J Raman Spectrosc 1994;25:75–87.
16. Cheng C, Kirkbride TE, Batchelder DN, Lacey RJ, Sheldon TG. In situ detection and identification of trace explosives by Raman microscopy. J Forensic Sci 1995;40:31–7.
17. Hayward IP, Kirkbride TE, Batchelder DN, Lacey RJ. Use of a fiber optic probe for the detection and identification of explosive materials by Raman spectroscopy. J Forensic Sci 1995;40:883–4.
18. Lewis IR, Daniel NW, Chaffin NC, Griffiths PR, Tungol MW. Raman spectroscopic studies of explosive materials towards a fieldable explosive detector. Spectrochim Acta 1995;51A:1985–2000.
19. Pestaner JP, Mullick FG, Centeno JA. Characterization of acetaminophen: molecular microanalysis with Raman microprobe spectroscopy. J Forensic Sci 1996;41:1060–3.
20. Coupry C, Brissaud D. Raman microscopy: applications in art, jewelry and forensic science. In: Turrell G, Corset J, editors. Raman microscopy: developments and applications. New York: Academic Press, 1996; 421–50.
21. Tsuchihashi H, Katagi M, Nishikawa M, Tatsuno M, Nishioka H, Nara A, Nishio E, Petty C. Determination of methamphetamine and its related compounds using Fourier transform Raman spectroscopy. Appl Spectrosc 1997;51:1796–9.
22. Keen IP, White GW, Fredericks PM. Characterization of fibers by Raman microprobe spectroscopy. J Forensic Sci 1998;43:82–9.
23. Sands HS, Hayward IP, Kirkbride TE, Bennett R, Lacey RJ, Batchelder DN. UV-excited resonance Raman spectroscopy of narcotics and explosives. J Forensic Sci 1998;43:509–13.
24. Ryder AG, O'Connor GM, Glynn TJ. Identifications and quantitative measurements of narcotics in solid mixtures using near-IR Raman spectroscopy and multivariate analysis. J Forensic Sci 1999;44: 1013–9.
25. Wilson AS, Edwards HGM, Farwell DW, Janaway RC. Fourier transform Raman spectroscopy: evaluation as a non-destructive technique for studying the degradation of human hair from archaeological and forensic environments. J Raman Spectrosc 1999;30:367–73.
26. Ellis G, Claybourn M, Richards SE. The applications of Fourier transform Raman spectroscopy to the study of paint systems. Spectrochim Acta 1990;46A:227–41.
27. Singer BW, Gardiner DJ, Derow JP. Analysis of white and blue pigments from watercolors by Raman microscopy. The Paper Conservator 1993;17:13–9.
28. Burgio L, Clark RJH, Gibbs PJ. Pigment identification studies in situ of Javanese, Thai, Korean, Chinese and Uighur manuscripts by Raman microscopy. J Raman Spectrosc 1999;30:181–4.
29. Edwards HGM, Farwell DW, Rozenberg S. Raman spectroscopic study of red pigment and fresco fragments from King Herod's palace at Jericho. J Raman Spectrosc 1999;30:361–6.
30. Zuo J, Xu C, Wang C, Yushi Z. Identification of the pigment in painted pottery from the Xishan site by Raman microscopy. J Raman Spectrosc 1999;30:1053–5.
31. Burgio L, Clark RJH, Stratoudaki T, Doulgeridis M, Anglos D. Pigment identification in painted artworks: A dual analytical approach employing laser-induced breakdown spectroscopy and Raman microscopy. Appl Spectrosc 2000;54:463–9.
32. Suzuki EM. Infrared spectra of U.S. automobile original topcoats (1974–1989): I. Differentiation and identification based on acrylonitrile and ferrocyanide C≡N stretching absorptions. J Forensic Sci 1996;41: 376–92.
33. Suzuki EM. Infrared spectra of U.S. automobile original topcoats (1974–1989): II. Identification of some topcoat inorganic pigments using an extended range (4000-220 cm^{-1}) Fourier transform spectrometer. J Forensic Sci 1996;41:393–406.
34. Lin-Vien D, Bland BJ, Spence VJ. An improved method of using the diamond anvil cell for infrared microprobe analysis. Appl Spectrosc 1990;44:1227–8.
35. Suzuki EM. Fourier transform infrared analyses of some particulate drug mixtures using a diamond anvil cell with a beam condenser and an infrared microscope. J Forensic Sci 1992;37:467–87.
36. Collaborative Testing Services, Inc. Reference collection of automotive paints technical data. Herndon, VA: Collaborative Testing Services, Sept. 1989.
37. Suzuki EM, Marshall WP. Infrared spectra of U.S. automobile original topcoats (1974–1989): III. In situ identification of some organic pigments used in yellow, orange, red, and brown nonmetallic and brown metallic finishes—benzimidazolones. J Forensic Sci 1997;42:619–48.
38. Suzuki EM, Marshall WP. Infrared spectra of U.S. automobile original topcoats (1974–1989): IV. Identification of some organic pigments used in red and brown nonmetallic and metallic monocoats—quinacridones. J Forensic Sci 1998;43:514–42.
39. Suzuki EM. Infrared spectra of U.S. automobile original topcoats (1974–1989): V. Identification of organic pigments used in red nonmetallic and brown nonmetallic and metallic monocoats—DPP Red BO and Thioindigo Bordeaux. J Forensic Sci 1999;44:297–313.
40. Suzuki EM. Infrared spectra of U.S. automobile original topcoats (1974–1989): VI. Identification and analysis of yellow organic automotive paint pigments—Isoindolinone Yellow 3R, Isoindoline Yellow, Anthrapyrimidine Yellow, and miscellaneous yellows. J Forensic Sci 1999;44:1151–75.
41. Bowie BT, Chase B, Griffiths PR. Factors affecting the performance of bench-top Raman spectrometers. Part I: instrumental effects. Appl Spectrosc 2000;54:164A–73A.
42. Rodgers PG, Cameron R, Cartwright NS, Clark WH, Deak JS, Norman EWW. The classification of automotive paint by diamond window infrared spectrophotometry. Part I: binders and pigments. Can Soc Forensic Sci J 1976;9:1–14.
43. Gothard JA. Evaluation of automotive paint flakes as evidence. J Forensic Sci 1976;21:636–41.
44. Ryland SG, Kopec RJ. The evidential value of automobile paint chips. J Forensic Sci 1979;24:140–7.

Additional information and reprint requests:
Ed Suzuki
Washington State Crime Laboratory
Public Safety Building, 2nd Floor
Seattle, WA 98104
E-Mail address: FTIRUser@aol.com